Published in final edited form as:
Neuroimage. 2012 May 1; 60(4): 2107–2117. doi:10.1016/j.neuroimage.2012.02.013.

Quantitative Imaging of Energy Expenditure in Human Brain

Xiao-Hong Zhu[1,*], **Hongyan Qiao**[1], **Fei Du**[1,3], **Qiang Xiong**[1,2], **Xiao Liu**[1,2], **Xiaoliang Zhang**[1,4], **Kamil Ugurbil**[1], and **Wei Chen**[1,2,*]

[1]Center for Magnetic Resonance Research, Department of Radiology, University of Minnesota Medical School, Minneapolis, MN 55455

[2]Department of Biomedical Engineering, University of Minnesota Medical School, Minneapolis, MN 55455

[3]McLean Hospital, Department of Psychiatry, Harvard Medical School, Belmont, Massachusetts

[4]Departments of Radiology and Bioengineering, University of California at San Francisco Medical School, California

Abstract

Despite the essential role of the brain energy generated from ATP hydrolysis in supporting cortical neuronal activity and brain function, it is challenging to noninvasively image and directly quantify the energy expenditure in the human brain. In this study, we applied an advanced *in vivo* ^{31}P MRS imaging approach to obtain regional cerebral metabolic rates of high-energy phosphate reactions catalyzed by ATPase (CMR_{ATPase}) and creatine kinase (CMR_{CK}), and to determine CMR_{ATPase} and CMR_{CK} in pure grey mater (GM) and white mater (WM), respectively. It was found that both ATPase and CK rates are three times higher in GM than WM; and CMR_{CK} is seven times higher than CMR_{ATPase} in GM and WM. Among the total brain ATP consumption in the human cortical GM and WM, 77% of them are used by GM in which approximately 96% is by neurons. A single cortical neuron utilizes approximately 4.7 billion ATPs per second in a resting human brain. This study demonstrates the unique utility of *in vivo* ^{31}P MRS imaging modality for direct imaging of brain energy generated from ATP hydrolysis, and provides new insights into the human brain energetics and its role in supporting neuronal activity and brain function.

Keywords

human brain; adenosine triphosphate (ATP); brain energy; *in vivo* ^{31}P MRS; ^{31}P magnetization transfer; cerebral metabolic rate of ATP production

Introduction

Cellular energy metabolism is a fundamental process that underlies and enables all the biological functions within a living organism. Adenosine triphosphate (ATP), which mainly formed in mitochondria through coupled electron transport chain and F_1F_0-ATPase

[*] **Correspondence Author:** Xiao-Hong Zhu, PhD or Wei Chen, PhD Center for Magnetic Resonance Research, Department of Radiology University of Minnesota School of Medicine 2021 6th Street S.E., Minneapolis, MN 55455 Phone: (612) 626-2001 Fax: (612) 626-2004 zhu@cmrr.umn.edu or wei@cmrr.umn.edu.

(ATPase) enzyme activities (i.e., the oxidative phosphorylation process), provides the chemical energy for virtually all energy-dependent cellular processes. In the brain, a majority of energy generated from ATP hydrolysis is utilized in the cytosol for supporting ongoing neuronal activity at resting state and elevated neuronal activity during a working state (Attwell and Laughlin, 2001; Erecinska and Silver, 1989; Raichle and Mintun, 2006; Shulman et al., 2004). Therefore, determining the rate of ATP hydrolysis is critical for understanding the bioenergetics of human brain at both normal and abnormal (i.e., diseased) conditions.

The energy demand in the human brain is not uniform and it is expected to be higher in the cortical grey matter (GM) than that of white matter (WM) based on the fundamental premise that GM tissue, characterized with high populations of synapses and mitochondria and intensive neuronal activity, needs more energy compared to the WM even though WM is intricately involved in signal transduction. Direct experimental verification of this premise, however, is limited by the availability of quantitative neuroimaging approaches capable of directly and noninvasively assessing the ATP metabolism and its rate with adequate spatial resolution for differentiating GM and WM in the human brain.

So far, most studies aiming for understanding the human brain energetics were commonly based on indirect neuroimaging measurements of cerebral metabolic rate of glucose (CMR_{glc}) or oxygen ($CMRO_2$) consumption for estimating the ATP utilization rate in the brains. These estimations rely on two hypothetical parameters: the molar ratio of oxygen consumption to glucose uptake (i.e., the oxygen-glucose index OGI) and the cerebral ATP synthesis to oxygen consumption ratio (P/O ratio). However, large uncertainties in determining the actual values of the OGI and P/O ratios in the human brain could result in substantial errors in estimating the cerebral metabolic rate of ATP. Theoretically, one glucose molecule will react with six oxygen molecules through oxidative metabolism and form 36 ATP molecules, leading to an OGI of 6 and P/O ratio of 3. Nevertheless, the OGI value measured by PET in the healthy human brain at resting state was lower than 6 and also not uniform across brain. For example, the OGI was reported to be ranging from 4.5 to 5.9 at different human brain regions (Vaishnavi et al., 2010), and it was also reported to be 4.1 in the human visual cortex at rest and dropped to 2.8 during visual stimulation (Fox et al., 1988). Moreover, the P/O ratio has been reported to be ≤ 2.5 (Du et al., 2008; Hinkle, 2005; Kingsley-Hickman et al., 1987; Zhu et al., 2002) apparently due to substantial proton leaking in the mitochondria (Rolfe and Brown, 1997). Therefore, ability to directly measure the cerebral metabolic rate of ATP production is essential for determining the true brain energy status associated with brain function or dysfunction. One available approach that in principle is capable of providing such information is the *in vivo* ^{31}P magnetic resonance (MR) spectroscopy (MRS) imaging.

In vivo ^{31}P MRS is a powerful tool for non-invasive detection of the intracellular contents of high-energy phosphate (HEP) compounds (e.g., ATP and phosphocreatine (PCr)) and inorganic phosphate (Pi) in the brain (e.g., (Kemp, 2000; Zhu et al., 2009), and references therein). The concentrations of HEP and Pi or their ratio can alter under pathological conditions; yet in normal brain, ATP production and utilization appear to be tightly regulated to maintain the HEP and Pi levels, in particular the ATP level, fairly constant across a wide range of physiological states where the brain activity level and associated ATP turnover rate can vary substantially (Du et al., 2008). Therefore, for assessing the cerebral energy metabolism and its effect on the brain function in healthy human brain, the measurement of HEP and Pi contents *per se* is not as informative as that of ATP metabolic rates (Du et al., 2008). The latter can be obtained using the *in vivo* ^{31}P MRS approach in combine with the magnetization transfer (MT) preparation (Forsen, 1963), which allows simultaneous measurement of two important *unidirectional* ATP production rates associated

with the creatine kinase (CK) (i.e., PCr→ATP) and ATPase (i.e., Pi→ATP) reactions in the brain, that are defined as cerebral metabolic rate of CK (CMR_{CK}) and ATPase (CMR_{ATPase}), respectively ((Du et al., 2007; Lei et al., 2003a) and references therein). Early attempts of using *in vivo* ^{31}P MRS-MT in the brain largely focused on measuring CMR_{CK} (Bottomley and Hardy, 1992; Shoubridge et al., 1982) given the relatively high intracellular PCr content and better MRS signal in the brain. The CK reaction, however, plays only a supportive role in facilitating ATP metabolism. A direct measure of net ATP production in the brain cell should be obtained through CMR_{ATPase}. However, *in vivo* measurement of CMR_{ATPase} faces a daunting challenge owing to a low intracellular Pi concentration (~ 1mM) and limited Pi signal change induced by the MT and chemical exchange effects in the brain, a major signal source for measuring the value of CMR_{ATPase}.

Recently, with the advancement in high-field MRI/MRS technology and relevant methodology development, it has been shown that CMR_{ATPase} can be reliably measured in the human occipital lobe using the *in vivo* ^{31}P MRS-MT approach and a radio-frequency (RF) surface coil at 7 Tesla (T) (Du et al., 2007; Lei et al., 2003a). Moreover, the CMR_{ATPase} values obtained in both human and animal brains were found to reflect the mitochondrial oxidative phosphorylation rates (Chaumeil et al., 2009; Du et al., 2007; Lei et al., 2003a; Shoubridge et al., 1982), and are sensitive to the variation in the basal brain activity in animal models cross a wide range of brain activity levels (Du et al., 2008). The previous human studies, however, measured CMR_{ATPase} from a small portion of the human brain located in the occipital lobe without spatial differentiation of GM and WM tissues (Du et al., 2007; Lei et al., 2003a).

In the present study, we have extended the utility of *in vivo* ^{31}P-MT approach by integrating three-dimensional (3D) chemical shift imaging (CSI), newly developed ^{1}H-^{31}P dual-frequency volume RF coil (Vaughan et al., 1994; Zhang et al., 2003) and a novel quantification strategy (Xiong et al., 2011) to quantitatively determine regional CMR_{ATPase} values of the human brain *in vivo* at 7T, ultimately, to: i) quantify and differentiate the cerebral ATP production rates in the grey and white matters of the human brain; ii) determine the energy expenditure differences between cortical GM and WM, and between neuron and non-neuronal cells; and iii) estimate the number of ATP molecules utilized per second by a single cortical neuron in a resting human brain.

Materials and Methods

Human Subject

Seven healthy volunteers (ages 20 to 34 years) from the University of Minnesota and local communities were recruited for the study. The Institutional Review Board at the University of Minnesota approved all procedures, and written informed consents were obtained from all subjects.

MRI/MRS Scanner and RF Coil

All studies were performed on a 7T/90cm magnet (Magnex Scientific, Abingdon, U.K.) interfaced with a Varian (Varian Inc., Palo Alto, CA, USA) INOVA console. A circular-polarized ^{1}H-^{31}P double-tuned TEM volume RF coil was constructed (Vaughan et al., 1994; Zhang et al., 2003). For the ^{31}P and ^{1}H measurements, the averaged RF power delivered through the coils were monitored and controlled at well below the FDA specific absorption rate (SAR) limit.

^{1}H MRI and Brain Tissue Segmentation

Anatomic images were obtained by T_1-weighted multi-slice TurboFLASH sequence (Haase et al., 1986) (inversion-recovery time: 1.2 s, repetition and echo times: TR/TE=8.8/3.9 ms; matrix size: 128×128; slice thickness: 5 mm) with whole brain coverage, and they were processed and segmented using the tools from the FMRIB (Oxford Centre for Functional Magnetic Resonance Imaging of the Brain) Software Library (www.fmrib.ox.ac.uk/fsl). Non-brain (e.g., scalp) regions were first removed using an automated brain extraction tool (BET) (Smith, 2002); and then three tissue types of grey matter, white matter and cerebrospinal fluid (CSF) were segmented using an automatic segmentation tool (FAST), which is based on a hidden Markov random field model and an associated Expectation-Maximization (EM) algorithm (Zhang et al., 2001). The fractional tissue contribution of grey-matter (f_{GM}) and white-matter (f_{WM}) to a particular ^{31}P-CSI voxel was calculated based on the corresponding segmented ^{1}H MRI data and the coordinates/dimensions of a selected ^{31}P-CSI voxel.

3D ^{31}P-MT CSI Measurement

3D ^{31}P-MT CSI data were acquired using the Fourier Series Window (FSW) CSI technique (Hendrich et al., 1994) in which the k-space sampling is weighted according to the Fourier coefficients of a predetermined voxel shape, thus, the data was oversampled in central k-space with partial truncation of higher k-space lines. Following acquisition parameters were used: 5000 Hz spectral bandwidth; nominal excitation pulse flip angle of β=36° with a 500-μs hard pulse; 20×20×22cm^3 field of view (FOV); 15×15×13 phase encodes; 1269 k-space lines; 3888 total scan number; 0.73 s TR; cylindrical voxel (circular shape on the transverse orientation and 2.4 cm diameter) with 10.9 ml actual (or 2.3 ml nominal) voxel size; and total acquisition time of 47.3 minutes per 3D CSI dataset. A frequency-selected saturation pulse train, constructed with multiple hyperbolic Sech pulses (pulse duration of 50 ms; bandwidth of 150 Hz) with varying amplitude according to the B_1 insensitive selective train to obliterate signal (BISTRO) scheme (de Graaf et al., 1996; Lei et al., 2003a) was incorporated into 3D ^{31}P FSW-CSI. The BISTRO pulse train was applied for frequency-selective saturation of the γ-ATP resonance peak for measuring the chemical exchange and MT effects on the magnetization (M_s) of PCr (or Pi); it was also applied at the mirror frequency of γ-ATP with respect to PCr for measuring control magnetization (M_c) under steady-state condition. During the data acquisition, subjects were instructed to relax and remain head still.

The ^{31}P-MT CSI data from selected voxels were analyzed in the time domain using the JMRUI software package (Version 3.0, available at http://www.mrui.uab.es) and the AMARES fitting algorithm (Vanhamme et al., 1997). The integrals of the ATP, PCr and intracellular Pi NMR signals obtained at control (M_c) and during saturation (M_s) were quantified for each CSI voxel. Tissue pH was also determined using the chemical shift difference between the intracellular Pi and the PCr resonances.

Quantification of Phosphate Metabolite Concentration

The relative concentrations of ATP, PCr and Pi metabolites were determined from their control magnetization M_c values after correcting for the saturation factor due to the short TR used for the CSI acquisition at 7T (Lei et al., 2003b). Absolute concentrations of PCr and Pi were then calculated using an average cerebral ATP concentration of 3 mM as an internal reference for each subject. This assumption is based on the fact that the cerebral ATP content under normal physiological condition is fairly constant as shown in the literature (Du et al., 2007; Du et al., 2008; Lei et al., 2003a).

Quantification of forward reaction rate constant with short TR acquisition

For the conventional ^{31}P-MT measurement under fully relaxed condition, there is a simple relation between the M_0/M_{ss} ratio and the forward reaction rate constant (k_f) according to:

$$M_0/M_{ss}=1+k_f \cdot T_1^{int} \quad [1]$$

where M_0 and M_{ss} are the fully relaxed magnetization at control and saturation and steady-state condition with adequately long saturation of γ-ATP, respectively; T_1^{int} is the intrinsic longitudinal relaxation time (T_1) of PCr for the CK reaction or Pi for the ATPase reaction in the absence of chemical exchange, and it can be treated as constant at a given magnetic field and has been measured in the human brain at 7T (Du et al., 2007; Lei et al., 2003a). In the present work, a short TR (TR < 1s) was used for the MT-CSI data acquisition in order to collect all desired k-space lines in 3D within a reasonable sampling time. Under this circumstance, Equation [1] does not hold anymore due to the confounding saturation contributions from short TR and chemical exchange MT effect. To overcome this challenge, a novel quantification method has been developed using a similar linear relation of

$$M_c/M_s \approx 1+k_f \cdot T_1^{nom} \quad [2]$$

where M_c and M_s are the control and γ-ATP-saturated magnetizations acquired with a short TR under steady-state condition; and T_1^{nom} is a nominal T_1 and depends on specific experimental parameters and magnetic field strength (Xiong et al., 2011). The T_1^{nom} values for the CK or ATPase reactions were derived via numerical simulation using the modified Bloch-McConnell equations incorporating three-site (i.e., PCr↔ATP↔Pi) chemical exchange model and known PCr/ATP/Pi concentration ratios as well as TR, flip angle β and the T^{int}_1 values measured at 7T (Du et al., 2007; Lei et al., 2003a; Xiong et al., 2011). Similar T^{int}_1 values for GM and WM were assumed. The major merit of this simple and robust T_1^{nom} quantification method is that it is generic and suitable for various TR and β values.

Quantification of CMR_{CK} and CMR_{ATPase}

The cerebral metabolic rate of CK and ATPase reactions can be quantified as $CMR_{CK} = k_{f,CK} \times [PCr]$ and $CMR_{ATPase} = k_{f,ATPase} \times [Pi]$; respectively. Once the absolute concentrations of PCr and Pi, as well as the forward rate constants of $k_{f,CK}$ and $k_{f,ATPase}$ are measured, one can readily determine the CMR_{CK} and CMR_{ATPase} values from any selected voxel or averages within a volume of interest (VOI) consisting of multiple selected voxels.

The RF volume coil was designed to cover the entire human brain with optimal sensitivity and B_1 homogeneity. The focus of this study was to differentiate the energy expenditure in different brain tissues, therefore, the VOIs were selected only from the cortical GM and WM regions with minimal B_0 inhomogeneity.

The conventional metabolic rate unit of μmol/g/min was used for presenting the ATP metabolic rates; brain tissue density of 1.1 g/ml was used for the purpose of unit conversion.

Statistical Analysis

All measurement results are presented as Mean±SD. Unpaired two-tail student's *t* test was applied for statistical analysis of the experimental data and a p value of < 0.05 is considered to be statistically significant.

Results

Three-dimensional ^{31}P-MT CSI of Human Brain at 7T

A ^{1}H-^{31}P dual-frequency volume RF coil with whole brain coverage was built and employed for collecting ^{1}H anatomic images and *in vivo* ^{31}P MRS/CSI data from healthy human subjects at 7T. Figure 1 demonstrates ^{1}H/^{31}P brain data obtained from a representative subject. The global brain ^{31}P spectra with only 4 signal averages were acquired using the pulse-acquisition sequence in the absence (Fig. 1a, control spectrum) and presence (Fig. 1b, saturated spectrum) of frequency-selective saturation on γ-ATP resonance. Excellent spectral quality and sensitivity offered by the high magnetic field are evident. Examples of control (Fig. 1d) and saturated (Fig. 1e) ^{31}P-MT CSI spectra extracted from the 3D dataset for a transverse plane are shown as two-dimensional (2D) plots together with the corresponding ^{1}H anatomic image (Fig. 1c). A multi-slice ^{1}H-^{31}P MR imaging dataset covering the whole brain can be found in **Supplementary Material** (Figure S1). These data demonstrate the full signal coverage of the ^{1}H-^{31}P head-volume RF coil and indicate that the 3D ^{31}P chemical shift images were spatially well matched with the corresponding ^{1}H anatomic images. Uniform B_1 field for ^{31}P RF excitation and signal reception are also evident in Fig. 1 and Figure S1 showing uniform ^{31}P signal distribution. Complete saturation of the γ-ATP resonance across the entire brain was achieved with the BISTRO saturation approach (de Graaf et al., 1996).

Figure 1 also displays the ^{31}P-MT spectral quality of single CSI voxel data (Fig. 1f and 1g, see Fig. 1c for the voxel location), where major resonance peaks of PCr, α-, γ-ATP, Pi and other metabolites related to cell membrane metabolism are well resolved and easily identified. In addition, in the selected GM-dominated voxel, it is obvious that the saturation of γ-ATP resonance (Fig. 1g) resulted in significant magnetization reductions for both PCr and Pi signals compared to the control spectrum (Fig. 1f) due to the chemical exchanges between these moieties. These reductions determine the values of CMR_{ATPase} and CMR_{CK}.

GM/WM-like VOI Selection and Brain Tissue Segmentation

Anatomical images were employed to select multiple ^{31}P voxels that can be divided into two categories: one located in a GM-dominated brain region and another in a WM-dominated region. Specifically, eight voxels were selected from either GM- or WM-dominated brain regions and grouped to form GM-like and WM-like VOI, respectively. The ^{31}P-MT spectra of those individual voxels within each VOI were then added together to form two averaged ^{31}P-MT spectra (one control and another saturated). Figure 2a shows an example of typical paired ^{31}P-MT spectra of the GM-like and WM-like VOIs from a representative subject. Compared to the single voxel spectra shown in Figs. 1f and 1g, Fig. 2a clearly demonstrates substantial improvements in spectral quality and the signal-to-noise ratio of the ^{31}P MRS signals of interest for quantification of brain phosphate contents and turnover rates CMR_{ATPase} and CMR_{CK}.

For each of the selected voxels, segmentation of the T_1-weighted ^{1}H MR images was performed to quantify the fractions of GM, WM and CSF compartments. Figure 2b shows one example of the segmented multi-slice ^{1}H MR images in which GM, WM and CSF were displayed in the composite images. The black circles (in top row images) and grey circles (in bottom row images) identified the selected GM- and WM-dominated voxels that formed the GM-like and WM-like VOIs. The segmentation result of this representative subject indicated that the GM-like VOI contained 59.2% GM, 26.4% WM and 14.4% CSF; while the WM-like VOI contained 87.5% WM, 11.0% GM and 1.5% CSF. The values of f_{GM} and f_{WM} obtained from different voxels and subjects were applied to estimate the CMR_{CK} and CMR_{ATPase} values in the pure grey and white matters based on linear regression.

CMR_{CK} and CMR_{ATPase} of Grey and White Matter

The 3D ^{31}P-MT CSI approach was applied in this study to measure the magnetizations of PCr and Pi at control (M_c) and γ-ATP saturation (M_s) conditions with *a short repetition time* in order to complete the entire CSI data acquisition within a reasonable time. Under this circumstance, the observed PCr and Pi signal reductions under steady-state condition rely not only on the exchange rates (or fluxes) but also on the saturation effect caused by the competition between the longitudinal relaxation time (T_1) and the allowed recovery time (i.e., TR), which leads to a complication on quantifying the apparent unidirectional rate constants of CK ($k_{f,CK}$) and ATPase ($k_{f,ATPase}$) reactions in the ATP synthesis direction. In this study, we applied the newly developed T_1^{nom} quantification method (see **Materials and Methods** and the reference of (Du et al., 2007; Lei et al., 2003a; Xiong et al., 2011) for detail) for overcoming this challenge. The T_1^{nom} values for CK or ATPase reactions were determined based on modeling and simulation results in which study-specified repetition time (TR=0.73s), RF excitation flip angle (β=36°) and the known intrinsic longitudinal relaxation time (T_1^{int}) values of PCr (4.9 s) and Pi (3.8 s) previously measured from the human brain at 7T (Du et al., 2007; Lei et al., 2003a) were used. Figure 3 presents the simulation results for both CK and ATPase reactions for the human brain application at 7T. Regression of the simulated data (circle or diamond points in Fig. 3) reveals that a strong linear correlation exists between the magnetization ratio (M_c/M_s) and the forward reaction rate constant (k_f) for both reactions with a correlation coefficient close to 1 ($R^2 > 0.999$). The slopes of the linear fitting were defined as T_1^{nom}, which were 3.10 s and 2.45 s for the forward CK and ATPase reaction, respectively. With experimentally measured magnetization ratio (M_c/M_s) and the T_1^{nom} constants, the forward reaction rate constants $k_{f,CK}$ and $k_{f,ATPase}$ can be readily calculated for the selected GM-like and WM-like VOIs in each subject according to Equation [2].

The cerebral metabolic rates of CMR_{CK} and CMR_{ATPase} can be calculated from the rate constants of $k_{f,CK}$ and $k_{f,ATPase}$ and the concentration of PCr and Pi, respectively. Table 1 summarizes the measurement results of VOI tissue fractions: f_{GM} and f_{WM}, [PCr] and [Pi], $k_{f,CK}$ and $k_{f,ATPase}$, and the cerebral metabolic rates of CMR_{CK} and CMR_{ATPase} in the GM-like and WM-like VOIs averaged from seven subjects. It shows that [PCr], $k_{f,CK}$ and $k_{f,ATPase}$, as well as CMR_{CK} and CMR_{ATPase} are significantly higher in the GM-like VOIs compared with those in the WM-like VOIs.

To correct the partial volume effect in the GM-like and WM-like VOIs, and to deduce the cerebral energy metabolisms in the pure GM and WM, a linear regression was performed for the CMR_{CK} and CMR_{ATPase} values in the GM-like and WM-like VOIs against their GM and WM fractions. As shown in Fig. 4, the linear regression resulted in 68.8±13.3 and 22.2±7.5 μmol/g/min for $CMR_{CK,GM}$ and $CMR_{CK,WM}$, 9.5±3.4 and 3.0±2.3 μmol/g/min for $CMR_{ATPase,GM}$ and $CMR_{ATPase,WM}$, respectively, yielding a GM/WM ratio of 3.2 for the ATPase reaction (i.e., CMR_{ATPase}) and 3.1 for the CK reaction (i.e., CMR_{CK}) in the resting healthy human brain.

In addition, we found that the GM-like VOIs displayed a slightly higher intracellular pH (7.025±0.013) than that of the WM-like VOIs (6.993±0.007) ($p<0.00001$, n=7), which lead to pH of 7.06 and 6.99 for the pure grey and white matter, respectively. In contrast, comparison of ATP contents based on the averaged integrals of γ-ATP and α-ATP signals between the GM-like and WM-like VOIs showed no significant difference ($p>0.2$, n=7).

Discussion

Feasibility for Differentiating ATP Energy Metabolism in Human Brain

In this study, we investigated ATP metabolic rates in the human brain using *in vivo* ^{31}P MRS imaging and magnetization transfer approaches at the ultrahigh field of 7T, and a volume RF head coil for both ^{31}P and ^{1}H data acquisition. When employ a volume RF coil, the sensitivity for detecting ^{31}P MRS signal maybe lower compared to a surface RF coil; however, large coverage and uniform ^{31}P RF pulse excitation across the entire brain achievable with the volume coil eliminated complications for quantifying CMR_{ATPase} and CMR_{CK}. Whole brain coverage is essential for regional differentiation of ATP energy metabolism associated with human brain function and/or diseases. Further improvements in sensitivity for whole brain coverage should be feasible by using a multichannel receive array.

With large brain coverage, an extended measurement time is inevitable for collecting the *in vivo* ^{31}P signals from the entire human brain, even when a much shorter repetition time is applied. In our study, this limitation was partially ameliorated with the substantial ^{31}P sensitivity gain available at the high field of 7T compared to clinically available magnetic fields up to 3T (Lei et al., 2003b; Qiao et al., 2006). After carefully selecting the optimal acquisition parameters, we were able to complete all MRI/MRS measurements within a reasonable time frame (~2 hrs) for the human study. Figure 1 reveals that adequate sensitivity and spatial resolution was achievable for 3D whole-brain ^{31}P-MT CSI measurements at 7T, which in turn made it possible to differentiate and determine the metabolic rates of CMR_{ATPase} and CMR_{CK} in the cortical grey and white matters of the human brain.

Novel Method for Quantifying ATP Metabolic Rates

When a much shorter repetition time (TR<1s) is used, as the present study, conventional ^{31}P-MT methods for quantifying reaction rate constants are no longer applicable. To overcome this limitation, we have developed a new strategy. A numerical simulation based on the Bloch-McConnell equations and field dependent T_1^{int} parameters of human brain at 7T predicted a linear relationship between the steady-state magnetization ratio (M_c/M_s) obtained with a short TR ^{31}P-MT CSI and the forward reaction rate constant (k_f). This linear relationship holds for a wide range of acquisition parameters (i.e., TR, flip angle β etc.) though the slope (i.e., T_1^{nom}) can vary. The acquisition parameters used in this study were in this linear regime (Fig. 3), which ensured reliable and robust determination of T_1^{nom} and accurate quantification of rate constants $k_{f,CK}$ and $k_{f,ATPase}$, and, ultimately, metabolic rates of CMR_{ATPase} and CMR_{CK}. This simple quantification method opens a door for many *in vivo* ^{31}P-MT applications.

To evaluate the validity and accuracy of this novel ^{31}P-MT imaging approach, we compared the ATP synthesis rates obtained in the present study with the CMR_{ATPase} values of healthy human brain that were either previously determined directly using the conventional ^{31}P-MT method in the human visual cortex (Du et al., 2007; Lei et al., 2003a) or indirectly estimated from the PET (Fox et al., 1988; Ito et al., 2004) and ^{13}C MRS (Boumezbeur et al., 2010; Gruetter et al., 2001; Shen et al., 1999) measurements. The comparison results are summarized in Table 2. They show that the CMR_{ATPase} values vary in certain degree depending on the imaging methods or brain regions that were obtained from; as well as the values of the conversion factors used in the calculation (see more discussion in the following section). However, the values of CMR_{ATPase} are generally consistent with relatively lower global brain values than that of the visual cortex or occipital-parietal lobes. This observation is in line with the findings of PET study showing both $CMRO_2$ and CMR_{glc} are significantly

higher in the primary visual cortex than the rest of the human (Fox et al., 1988). Therefore, the CMR_{ATPase} value obtained with the *in vivo* ^{31}P-MT CSI approach reflects the rate of cerebral oxidative phosphorylation of ADP, which determines the production rate of the brain energy via ATP hydrolysis; and the CMR_{ATPase} could serve as the most reliable and direct index of brain energy *in vivo*.

Distinct ATP Metabolic Rates between GM and WM in a Resting Human Brain

The strategy of combining MRS measurement with image segmentation to correct the metabolite heterogeneities due to tissue composition has been established for a while (Doyle et al., 1995; Hetherington et al., 2001) and it was applied in the present study. Through measuring the ATP production rates in the brain regions dominated by grey or white matter (i.e., GM-like or WM-like VOIs) and quantifying the grey/white matter compositions in those VOIs via image segmentation, the CMR_{ATPase} and CMR_{CK} values of pure GM or WM matter in the resting human brain were determined via a linear regression (Doyle et al., 1995; Hetherington et al., 2001). It was found that both CMR_{ATPase} and CMR_{CK} are approximately three times higher in GM ($CMR_{ATPase,GM}$ = 9.5 μmol/g/min and $CMR_{CK,GM}$ = 68.8 μmol/g/min) than that in WM ($CMR_{ATPase,WM}$ = 3.0 μmol/g/min and $CMR_{CK,WM}$ = 22.2 μmol/g/min). In contrast, the cellular ATP contents are similar between the GM and WM tissues despite the large difference in CMR_{ATPase} or CMR_{CK}. This observation is consistent with the view that a homeostasis of intracellular ATP concentration is essential for normal brain function. In animal studies, ATP content was found to be constant over a wide range of brain activity level from a state characterized by intensive spontaneous EEG to an iso-electric state with completely silent EEG activity (Du et al., 2008). Similar observations have been previously made in the heart as well, where under normal circumstances ATP is maintained constant over a large workload and oxygen consumption range (Balaban et al., 1986; From et al., 1990). Clearly, in these highly aerobic organs, an extremely efficient and rapid regulation must exist between ATP supply and demand for maintaining a constant ATP level.

ATP supply in the brain relies largely on the oxidative phosphorylation of ADP in mitochondria while the ATP utilization occurs in cytosol, predominantly to satisfy the neuronal energy demand. The rapid cycling between the ATP production and utilization requires extremely high efficiency for transportation of ATP, ADP and Pi between the sub-cellular compartments of mitochondria and the ATP consuming site in the cytosol. This function is facilitated in part by the fast CK reaction which provides an efficient “shuttle” between ATP producing and consuming sites (Wallimann et al., 1992). Consistent with this view, we found that CMR_{CK} is more than seven times higher than CMR_{ATPase} in both GM and WM of the human brain. Therefore, highly regulated and coupled ATPase and CK reactions are essential for maintaining a homeostasis of intracellular ATP concentration in the brain.

Energy Expenditure, Neuronal Activity and Brain function

The central role of ATP metabolism in supporting energy for neuronal activity and signaling is fully anticipated and recognized. However, going beyond this recognition to generating models and conclusions that provide quantitative relationships between neuronal signaling and energy expenditure (Attwell and Laughlin, 2001; Erecinska and Silver, 1989; Hyder et al., 2006; Raichle and Mintun, 2006; Shulman et al., 2004) relies on estimations based on indirect energy indices such as CMR_{glc} or $CMRO_2$ with a number of assumptions and conversion factors (e.g., see (Attwell and Laughlin, 2001) and references therein). Specifically, the CMR_{glc} and $CMRO_2$ can be imaged in the human brain using ^{18}F and ^{15}O labeled radioactive tracers, respectively, with the PET imaging modality (Mintun et al., 1984; Reivich et al., 1977) or be indirectly derived from the tricarboxylic acid (TCA) cycle

rate (V_{TCA}) determined using ^{13}C labeled carbohydrate substrate with *in vivo* ^{13}C MRS measurements (Gruetter et al., 2001; Rothman et al., 2011; Shulman et al., 2001). As we pointed out earlier, the conversion from CMR_{glc} and/or $CMRO_2$ to CMR_{ATPase} relies on the assumption that the actual values of OGI and/or P/O ratios are known; and the conversion of V_{TCA} to CMR_{ATPase} assumes that the ratio between V_{TCA} and CMR_{glc} or $CMRO_2$ is known as well. However, one should be cautious since these key conversion factors (e.g. OGI and P/O ratios) are hard to determine and their values could vary substantially among different species, conditions (normal or diseased), states (resting or working), and even different brain regions. For instance, the OGI value of temporal lobe was found to be >20% higher than that of prefrontal lobe in the human brain (Vaishnavi et al., 2010). Thus, one should be cautious in estimating CMR_{ATPase} using the conversion factors and CMR_{glc}, $CMRO_2$ or V_{TCA} value.

On the other hand, the ^{31}P-MT MRS or CSI approach could directly measure the rate of ATP hydrolysis that represents the actual energy expenditure of the brain tissue. The results of the present study could be used to quantitatively address the ATP energy questions in the human brain. These measured CMR_{ATPase} values of the human cortical GM and WM reflect the ATP production rates, which equal to the ATP utilization rates due to chemical equilibrium between forward and reversed ATPase reactions (Du et al., 2007). By incorporating knowledge of the cell densities of neurons (19.54 million/g-GM and 4.38 million/g-WM) and non-neuronal cells (27.44 million/g-GM and 67.57 million/g-WM) in the human cortical GM and WM (Azevedo et al., 2009), the results of CMR_{ATPase} determined in the cortical GM ($CMR_{ATPase,GM}$ = 9.5 μmol/g/min) and WM ($CMR_{ATPase,WM}$ = 3.0 μmol/g/min) in the present study were used to derive the human brain energy expenditure at the system level covering the entire cortical brain region and the GM/WM tissue compartments and at the cellular level of single neuron (detailed calculation can be found in **Appendix**). Since the CMR_{ATPase} results were experimentally measured and selectively quantified for the cerebral cortex regions of the human brain, thus, the energy calculation of present study focused only on the energy expenditures of the cortical GM and WM that account for approximately 82% of total human brain mass (Azevedo et al., 2009) with exclusion of cerebellum and sub-cortical region.

Human brain energy expenditures of cortical GM and WM—At the system level, we found that on average, the resting human cortical GM utilizes 6.01 mmole of ATP molecules per minute in comparison with 1.77 mmole of ATP per minute used by WM, and the total of human cortical GM and WM consumes 7.78 mmole of ATP each minute. Several important conclusions, therefore, can be drawn from these quantities in regards to cerebral ATP energetics in various tissue compartments.

First, the cortical GM utilizes approximately 77% of total energy expenditure of the cortical GM and WM tissues, though it only accounts 52% of total GM+WM tissue weight. This portion of energy generated from ATP hydrolysis is essential for supporting ongoing neuronal activities plus the “housekeeping” biological processes occurring in a resting awake human brain. This energy expenditure can become even higher in animal brains because of a much higher GM/WM volume ratio (e.g., ~3.5 for the cat brain and ~8 for the rat brain compared to 1.5 for the human brain (Ge et al., 2002; Zhang and Sejnowski, 2000)). This notion is consistent with the higher metabolic rates of $CMRO_2$ and CMR_{glc} commonly observed in awake animals (Siesjo, 1978).

Secondly, an enormous amount of ATP molecules (≈ *5.7 kg*) is produced and utilized by the human cortical GM and WM in a single day, which is equivalent to the complete oxidative combustion of 56 g glucose per day (assuming an ATP/glucose ratio of 36); and this ATP consumption amount is almost *five times* of the total weight of human cortical GM and WM (≈*1.2 kg*). It is clear that the ATP turnover rate in a normal brain has to be extremely high;

and the majority of the energy generated in the process is used by the cortical GM with a large population of neuronal cell bodies, dendrites and synapses and high densities of mitochondria and capillary. Such a high energy demand can be only satisfied by extremely efficient ATP production through oxidative phosphorylation in the mitochondria and rapid balance between ATP utilization and production.

Energy expenditures between neuron and non-neuronal cells—In general, the brain cells can be divided into two major categories: neurons and non-neuronal cells that mainly consist of glia cells including astrocytes. The cell densities are not uniform across the human brain. The ratio of the non-neuronal to neuron cell numbers is 1.4 in the human GM, and 15.4 in the human WM indicating a dominant cell population of non-neuronal cells in WM (Azevedo et al., 2009). As an approximation by assuming that the same type of cell (neuron or non-neuronal) utilizes a similar amount of ATP in different brain tissue (GM or WM), we estimated that a non-neuronal cell utilizes approximately 3% of energy generated from the ATP hydrolysis in a neuron cell in the human brain (see **Appendix**). Thus, neurons indeed are highly energy-consuming cells. More evidence in this regard is from the calculation results indicating that 96% of the total energy expenditure in the human cortical GM is utilized by neurons. These results are consistent with the histological finding that more than 90% of the total mitochondria in the primate visual cortex were found in the neurons, and only 2% were located inside glia (Rolfe and Brown, 1997; Wong-Riley et al., 1989). The majority of mitochondria inside the neurons locate in dendrites and synapses (Rolfe and Brown, 1997; Wong-Riley et al., 1989), suggesting extensive energy expenditure for interneuron signaling.

Interestingly, although only 6% of the cells in the human WM are neurons they still utilize 68% of the total energy attributed to the WM tissue. Nevertheless, the energy expenditure of non-neuronal cells becomes significant in WM and it can reach 32% as compared to 4% in cortical GM. For most neuroimaging measurements, the signals are likely contributed from both GM and WM tissues (so called partial volume effect), thus, the relative energy expenditure of non-neuronal cells is expected to be in a range from 4% as in the pure GM to 32% as in the pure WM tissue. As discussed in **Appendix**, the fractional energy expenditure of non-neuronal cells can reach 10% in the brain region with equally mixed GM and WM tissues, which is in line with the average result of fractional glial ATP synthesis contribution of ~11% based on *in vivo* ^{13}C MRS measurements in the healthy human brains (see the reviewer article by Rothman et al. (Rothman et al., 2011) and cited references therein).

Energy expenditure of a single cortical neuron—The energy expenditure of a single human cortical neuron was calculated to be 4.7 billion ATPs per second (i.e., 4.7×10^9 ATPs/neuron/s) after correcting the glia cell energy contribution to the total energy expenditure. This value is substaintially higher than that of 3.3×10^9 ATPs/neuron/s indirectly estimated for the rat brain (Attwell and Laughlin, 2001). Though the human neuron cell structure is similar with animal neurons, it has a relatively larger cell size with more synapses (Lennie, 2003), thus presumably, consuming more ATP molecules as observed in the present study. This energy expenditure is essential to support a variety of electrophysiological activities including resting potentials, spontaneous spiking (or action potential), neurotransmitter cycling as well as “housekeeping” power required for biosynthesis, enzyme activities and maintenance of tissue integrity (Attwell and Laughlin, 2001; Du et al., 2008; Hyder et al., 2006; Lennie, 2003). The “housekeeping” energy requirement in an awake human brain is unknown, it was speculated to be in the range of one quarter to one third of total energy expenditure based on animal studies (Du et al., 2008; Hyder et al., 2006; Rolfe and Brown, 1997). If this ratio is applicable for the human brain, then approximately 67-75% of the total neuronal energy expenditure (i.e., 3.1×10^9 to 3.5×10^9 ATPs/neuron/s) is used for

neurotransmitter signaling and electrophysiological activities that are crucial for maintaining ongoing neuronal activity and normal brain function under the resting state.

Energy expenditure in the resting and working states—From the perspective of neuroenergetic and neurovascular couplings, the extremely high ATP demand in the human cortex should correlate to higher oxygen and glucose metabolic rates and blood flow, in particular, commonly observed in the human cortical GM regions (Attwell and Laughlin, 2001; Raichle and Mintun, 2006; Shulman et al., 2004). The high metabolic activities (e.g., $CMRO_2$ and CMR_{glc}) and blood flow and their dynamic changes provide the major signal sources for most noninvasive neuroimaging modalities used for mapping ongoing neuronal activity fluctuations, functional connectivity, and neural networks in a "resting" brain (Biswal et al., 1995; Fox and Raichle, 2007), or obtaining functional activation maps of task- and stimulus-evoked neuronal activity change in a "working" brain (Bandettini et al., 1992; Kwong et al., 1992; Ogawa et al., 1992). Interestingly, one compelling phenomenon is that the main signal changes mapped by most neuroimaging modalities under either resting or working state are from the GM tissues. Our finding of a much higher rate of ATP hydrolysis in resting human cortical GM than that of WM links to this phenomenon in the perspective of neuroenergetics.

A direct comparison of the human brain energy expenditure between resting and working brain states is still challenging due to the lack of direct measurements of energy expenditure under both resting and working states. A few studies have provided indirect evidence suggesting a relatively small increment of brain energy expenditure during brain activation. For instance, an early PET study reported a few percents of $CMRO_2$ increase in the human visual cortex during visual stimulation (Fox et al., 1988). On the other hand, the majority of brain energy generated from ATP hydrolysis is probably utilized in the resting brain already. However, the definite answer to this question requires more research to quantify CMR_{ATPase} in both resting and activated human brain, for instance, using the advanced *in vivo* ^{31}P-MT CSI approach as demonstrated in the present study.

Conclusion

In summary, we demonstrate that the process of ATP production or consumption in human brain can be imaged non-invasively and partitioned into grey and white matter compartments from different locations in the human brain. The results reveal that both ATPase and creatine kinase activities are more than three folds higher in grey matter than that of white matter in a "resting" human brain. This study made it possible, for the first time, to directly measure and quantify the human brain energy expenditure from cellular (neuron and non-neuronal cell) to system (WM, GM and global brain) level. We expect the capability provided by the *in vivo* ^{31}P-MT neuroimaging approach and high-field human MRI/MRS technology as demonstrated herein could open a new frontier for quantitatively studying neuroenergetics and its change associated with brain function and dysfunction.

Supplementary Material

Refer to Web version on PubMed Central for supplementary material.

Acknowledgments

This work was supported in part by National Institute of Health grants: NS057560, NS41262, NS41262S1, NS070839, NS070839S1, HL050470, P41 RR08079 and P30 NS057091; and the WM KECK Foundation.

Appendix

Calculation of Human Brain Energy Expenditures

In the present study, the values of $CMR_{ATP,GM}$ (= 9.5 μmol/g/min) and $CMR_{ATP,WM}$ (= 3.0 μmol/g/min) were experimentally measured and quantified based on the selected brain tissues regions that mainly located in the cortical grey matter (GM) and white matter (WM) without inclusion of cerebellum and sub-cortical areas. Therefore, the following calculation focuses only on the human brain energy expenditures of the cortical GM and WM that constitute approximately 82% of total human brain mass (Azevedo et al., 2009). The brain cells are mainly divided into two types: neurons and non-neuronal cells including glia and astrocytes. Several important brain parameters taken from a recent publication (Azevedo et al., 2009) and other known constants were applied to the calculation:

- Cortical GM weight per hemisphere ($W_{h,GM}$): 316.3 g
- Cortical WM weight per hemisphere ($W_{h,WM}$): 294.2 g
- Total neuron number in GM per hemisphere ($N_{n,GM}$): 6.18 billon
- Total non-neuronal cell number in GM per hemisphere ($N_{nn,GM}$): 8.68 billon
- Total neuron number in WM per hemisphere ($N_{n,WM}$): 1.29 billon
- Total non-neuronal cell number in WM per hemisphere ($N_{nn,WM}$): 19.88 billon
- ATP molecular weight (MW_{ATP}) = 507 g/mole
- One mole compound has 6.02×10^{23} molecules.

Using these parameters, we can calculate following parameters:

- Total GM weight of two hemispheres ($W_{t,GM}=W_{h,GM}\times2$): 632.6 g
- Total WM weight of two hemispheres ($W_{t,WM}=W_{h,WM}\times2$): 588.4 g
- Total cortical GM and WM tissue weight ($W_{t,GM+WM}=W_{t,GM}+W_{t,WM}$): 1221 g
- Neuron cell density in GM ($D_{n,GM}=N_{n,GM}\div W_{h,GM}$=6.18 billion/316.3 g×1000): 19.54 million/g-GM
- Neuron cell density in WM ($D_{n,WM}=N_{n,WM}\div W_{h,WM}$=1.29 billion/294.2 g×1000): 4.38 million/g-WM
- Non-neuronal cell density in GM ($D_{nn,GM}=N_{nn,GM}\div W_{h,GM}$=8.68 billion/316.3 g×1000): 27.44 million/g-GM
- Non-neuronal cell density in WM ($D_{nn,WM}=N_{nn,WM}\div W_{h,WM}$=19.88 billion/294.2 g×1000): 67.57 million/g-WM

Human brain energy expenditures of cortical GM and WM

We can estimate the following brain energy expenditures:

- Cortical GM energy expenditure per minute ($E_{GM}=W_{t,GM}\times CMR_{ATP,GM}$ = 632.6 g×9.5 μmol/g/min=6010 μmol/min): 6.01 mmol/min
- Cortical WM energy expenditure per minute ($E_{WM}=W_{t,WM}\times CMR_{ATP,WM}$ =588.4 g×3.0 μmol/g/min=1765 μmol/min): 1.77 mmol/min
- Total energy expenditure of cortical GM and WM per minute ($E_{WM+WM}=E_{GM}+E_{WM}$): 7.78 mmol/min.

Therefore, a resting human brain will consume 5.7 kg ATP per day ($=E_{WM+WM}\times 24$ hour$\times 60$ min/hour$\times MW_{ATP}\times 10^{-6}$), which is approximately five times of total GM and WM tissue weight. The cortical GM utilizes 77% ($=E_{GM}\div E_{WM+WM}$) of total energy expenditure used by the cortical GM and WM tissues, though it only accounts 52% ($=W_{t,GM}\div W_{t,GM+WM}$) of total cortical GM+WM tissue weight.

Energy expenditures between neuron and non-neuronal cell

The same type of neuron or non-neuronal cells is assumed to approximately have a similar energy expenditure no matter where they located (in GM or WM). The energy expenditure ratio (R) between a single neuron and a single non-neuronal cell can be determined using the following formula:

$$CMR_{ATP,GM}\div CMR_{ATP,WM}=\left(1.0\times D_{n,GM}+R\times D_{nn,GM}\right)\div\left(1.0\times D_{n,WM}+R\times D_{nn,WM}\right)$$

which resulted in the value of R = 0.03. This result suggests that a non-neuronal cell only utilizes approximately 3% of that used by a neuron in the human brain. This value can be used to determine the following energy expenditures:

- Fraction of energy expenditure utilized by neurons in GM ($F_{n,GM}$) that equals to$1.0\times D_{n,GM}\div[1.0\times D_{n,GM}+R\times D_{nn,GM}]$, thus, $F_{n,GM}=0.96$ or 96%
- Fraction of ATP energy expenditure utilized by neurons in WM ($F_{n,WM}$) that equals to$1.0\times D_{n,WM}\div[1.0\times D_{n,WM}+R\times D_{nn,WM}]$, thus, $F_{n,GM}=0.68$ or 68%

These numbers indicate that the neurons in GM dominate the energy expenditure. In WM, neuron still utilize the majority of the energy generated from ATP hydrolysis, however, the energy expenditure of non-neuronal cells becomes significant of up to 32%.

For most neuroimaging measurements, the signals are likely contributed from both GM and WM tissues (so called partial volume effect), thus, the relative energy expenditure of non-neuronal cells will be between 4% as in the pure GM and 32% as in the pure WM tissue. One interesting demonstration of this point is to calculate the fractional energy expenditure of non-neuronal cells in the brain region with equally mixed GM and WM tissues using following formula:

$$=R\left(D_{nn,GM}+D_{nn,WM}\right)\div\left[R\left(D_{nn,GM}+D_{nn,WM}\right)+1.0\left(D_{n,GM}+D_{n,WM}\right)\right]$$
$$=0.102 \quad \text{or} \quad 10.2\%$$

Energy expenditure of a single cortical neuron

The measured $CMR_{ATP,GM}$ value of 9.5 μmol/g/min can be converted to: 9.5 μmol ATP/g-GM/min$\times 10^{-6}\times 6.02\times 10^{23}/60\text{s} = 9.53\times 10^{16}$ ATP/g-GM/s and 96% of this energy expenditure is to support the neurons in GM. Therefore, the energy expenditure of a single neuron can be calculated by $0.96\times 9.53\times 10^{16}$ ATP/g-GM/s$\div 19.54\times 10^{6}$ neuron/g-GM = 4.7×10^{9} ATPs/neuron/s, i.e, a single cortical neuron utilizes 4.7 billion ATPs per second.

Abbreviations

ATP	adenosine triphosphate
ADP	adenosine diphosphate
PCr	phosphocreatine

Pi	inorganic phosphate
HEP	high-energy phosphate
ATPase	F_1F_0-ATPase
CK	creatine kinase
MRS	magnetic resonance spectroscopy
MT	magnetization transfer
CMR_{ATPase}	forward ATPase reaction flux, also define as cerebral metabolic rate of ATPase
CMR_{CK}	forward CK reaction flux, also define as cerebral metabolic rate of CK

References

Attwell D, Laughlin SB. An energy budget for signaling in the grey matter of the brain. J Cereb Blood Flow Metab. 2001; 21:1133–1145. [PubMed: 11598490]

Azevedo FA, Carvalho LR, Grinberg LT, Farfel JM, Ferretti RE, Leite RE, Jacob Filho W, Lent R, Herculano-Houzel S. Equal numbers of neuronal and nonneuronal cells make the human brain an isometrically scaled-up primate brain. J Comp Neurol. 2009; 513:532–541. [PubMed: 19226510]

Balaban RS, Kantor HL, Katz LA, Briggs RW. Relation between work and phosphate metabolite in the in vivo paced mammalian heart. Science. 1986; 232:1121–1123. [PubMed: 3704638]

Bandettini PA, Wong EC, Hinks RS, Tikofsky RS, Hyde JS. Time course EPI of human brain function during task activation. Magn Reson Med. 1992; 25:390–397. [PubMed: 1614324]

Biswal B, Yetkin FZ, Haughton VM, Hyde JS. Functional connectivity in the motor cortex of resting human brain using echo-planar MRI. Magn Reson Med. 1995; 34:537–541. [PubMed: 8524021]

Bottomley PA, Hardy CJ. Mapping creatine kinase reaction rates in human brain and heart with 4 Tesla saturation transfer ^{31}P NMR. J. Magn. Reson. 1992; 99:443–448.

Boumezbeur F, Mason GF, de Graaf RA, Behar KL, Cline GW, Shulman GI, Rothman DL, Petersen KF. Altered brain mitochondrial metabolism in healthy aging as assessed by in vivo magnetic resonance spectroscopy. J Cereb Blood Flow Metab. 2010; 30:211–221. [PubMed: 19794401]

Chaumeil MM, Valette J, Guillermier M, Brouillet E, Boumezbeur F, Herard AS, Bloch G, Hantraye P, Lebon V. Multimodal neuroimaging provides a highly consistent picture of energy metabolism, validating ^{31}P MRS for measuring brain ATP synthesis. Proc Natl Acad Sci U S A. 2009; 106:3988–3993. [PubMed: 19234118]

de Graaf RA, Luo Y, Garwood M, Nicolay K. B_1-insensitive, single-shot localization and water suppression. Journal of Magnetic Resonance Series B. 1996; 113:35–45. [PubMed: 8888589]

Doyle TJ, Bedell BJ, Narayana PA. Relative concentrations of proton MR visible neurochemicals in gray and white matter in human brain. Magn Reson Med. 1995; 33:755–759. [PubMed: 7651110]

Du F, Zhu XH, Qiao H, Zhang X, Chen W. Efficient in vivo ^{31}P magnetization transfer approach for noninvasively determining multiple kinetic parameters and metabolic fluxes of ATP metabolism in the human brain. Magn Reson Med. 2007; 57:103–114. [PubMed: 17191226]

Du F, Zhu XH, Zhang Y, Friedman M, Zhang N, Ugurbil K, Chen W. Tightly coupled brain activity and cerebral ATP metabolic rate. Proc Natl Acad Sci U S A. 2008; 105:6409–6414. [PubMed: 18443293]

Erecinska M, Silver IA. ATP and brain function. J Cereb Blood Flow Metab. 1989; 9:2–19. [PubMed: 2642915]

Forsen S. Study of Moderately Rapid Chemical Exchange Reactions by Means of Nuclear Magnetic Double Resonance. The Journal of Chemical Physics. 1963; 39:2892–2901.

Fox MD, Raichle ME. Spontaneous fluctuations in brain activity observed with functional magnetic resonance imaging. Nat Rev Neurosci. 2007; 8:700–711. [PubMed: 17704812]

Fox PT, Raichle ME, Mintun MA, Dence C. Nonoxidative glucose consumption during focal physiologic neural activity. Science. 1988; 241:462–464. [PubMed: 3260686]

From AH, Zimmer SD, Michurski SP, Mohanakrishnan P, Ulstad VK, Thoma WJ, Ugurbil K. Regulation of the oxidative phosphorylation rate in the intact cell. Biochemistry. 1990; 29:3731–3743. [PubMed: 2340268]

Ge Y, Grossman RI, Babb JS, Rabin ML, Mannon LJ, Kolson DL. Age- related total gray matter and white matter changes in normal adult brain. Part I: volumetric MR imaging analysis. AJNR Am J Neuroradiol. 2002; 23:1327–1333. [PubMed: 12223373]

Gruetter R, Seaquist ER, Ugurbil K. A mathematical model of compartmentalized neurotransmitter metabolism in the human brain. Am J Physiol Endocrinol Metab. 2001; 281:E100–112. [PubMed: 11404227]

Haase A, Frahm J, Matthaei D, Hanicke W, Merboldt KD. FLASH imaging. Rapid NMR imaging using low flip angle pulses. J. Magn. Reson. 1986; 67:258–266.

Hendrich K, Hu X, Menon R, Merkle H, Camarata P, Heros R, Ugurbil K. Spectroscopic imaging of circular voxels with a two-dimensional Fourier-Series Window technique. J Magn Reson. 1994; 105:225–232.

Hetherington HP, Spencer DD, Vaughan JT, Pan JW. Quantitative ^{31}P spectroscopic imaging of human brain at 4 Tesla: assessment of gray and white matter differences of phosphocreatine and ATP. Magn Reson Med. 2001; 45:46–52. [PubMed: 11146485]

Hinkle PC. P/O ratios of mitochondrial oxidative phosphorylation. Biochim Biophys Acta. 2005; 1706:1–11. [PubMed: 15620362]

Hyder F, Patel AB, Gjedde A, Rothman DL, Behar KL, Shulman RG. Neuronal-glial glucose oxidation and glutamatergic-GABAergic function. J Cereb Blood Flow Metab. 2006; 26:865–877. [PubMed: 16407855]

Ito H, Kanno I, Kato C, Sasaki T, Ishii K, Ouchi Y, Iida A, Okazawa H, Hayashida K, Tsuyuguchi N, Kuwabara Y, Senda M. Database of normal human cerebral blood flow, cerebral blood volume, cerebral oxygen extraction fraction and cerebral metabolic rate of oxygen measured by positron emission tomography with 15O-labelled carbon dioxide or water, carbon monoxide and oxygen: a multicentre study in Japan. Eur J Nucl Med Mol Imaging. 2004; 31:635–643. [PubMed: 14730405]

Kemp GJ. Non-invasive methods for studying brain energy metabolism: what they show and what it means. Dev Neurosci. 2000; 22:418–428. [PubMed: 11111158]

Kingsley-Hickman PB, Sako EY, Mohanakrishnan P, Robitaille PM, From AH, Foker JE, Ugurbil K. ^{31}P NMR studies of ATP synthesis and hydrolysis kinetics in the intact myocardium. Biochemistry. 1987; 26:7501–7510. [PubMed: 3427090]

Kwong KK, Belliveau JW, Chesler DA, Goldberg IE, Weisskoff RM, Poncelet BP, Kennedy DN, Hoppel BE, Cohen MS, Turner R, Cheng HM, Brady TJ, Rosen BR. Dynamic magnetic resonance imaging of human brain activity during primary sensory stimulation. Proc Natl Acad Sci U S A. 1992; 89:5675–5679. [PubMed: 1608978]

Lei H, Ugurbil K, Chen W. Measurement of unidirectional Pi to ATP flux in human visual cortex at 7 T by using *in vivo* ^{31}P magnetic resonance spectroscopy. Proc Natl Acad Sci U S A. 2003a; 100:14409–14414. [PubMed: 14612566]

Lei H, Zhu XH, Zhang XL, Ugurbil K, Chen W. *In vivo* ^{31}P magnetic resonance spectroscopy of human brain at 7 T: an initial experience. Magn Reson Med. 2003b; 49:199–205. [PubMed: 12541238]

Lennie P. The cost of cortical computation. Curr Biol. 2003; 13:493–497. [PubMed: 12646132]

Mintun MA, Raichle ME, Martin WR, Herscovitch P. Brain oxygen utilization measured with O-15 radiotracers and positron emission tomography. J Nucl Med. 1984; 25:177–187. [PubMed: 6610032]

Ogawa S, Tank DW, Menon R, Ellermann JM, Kim SG, Merkle H, Ugurbil K. Intrinsic signal changes accompanying sensory stimulation: functional brain mapping with magnetic resonance imaging. Proc Natl Acad Sci U S A. 1992; 89:5951–5955. [PubMed: 1631079]

Qiao H, Zhang X, Zhu XH, Du F, Chen W. In vivo ^{31}P MRS of human brain at high/ultrahigh fields: a quantitative comparison of NMR detection sensitivity and spectral resolution between 4 T and 7 T. Magn Reson Imaging. 2006; 24:1281–1286. [PubMed: 17145398]

Raichle ME, Mintun MA. Brain work and brain imaging. Annu Rev Neurosci. 2006; 29:449–476. [PubMed: 16776593]

Reivich M, Kuhl D, Wolf A, Greenberg J, Phelps M, Ido T, Casella V, Fowler J, Gallagher B, Hoffman E, Alavi A, Sokoloff L. Measurement of local cerebral glucose metabolism in man with 18F-2-fluoro-2-deoxy-d-glucose. Acta Neurol Scand Suppl. 1977; 64:190–191. [PubMed: 268783]

Rolfe DF, Brown GC. Cellular energy utilization and molecular origin of standard metabolic rate in mammals. Physiol Rev. 1997; 77:731–758. [PubMed: 9234964]

Rothman DL, De Feyter HM, de Graaf RA, Mason GF, Behar KL. ^{13}C MRS studies of neuroenergetics and neurotransmitter cycling in humans. NMR Biomed. 2011; 24:943–957. [PubMed: 21882281]

Shen J, Petersen KF, Behar KL, Brown P, Nixon TW, Mason GF, Petroff OA, Shulman GI, Shulman RG, Rothman DL. Determination of the rate of the glutamate/glutamine cycle in the human brain by in vivo ^{13}C NMR. Proc Natl Acad Sci U S A. 1999; 96:8235–8240. [PubMed: 10393978]

Shoubridge EA, Briggs RW, Radda GK. 31P NMR saturation transfer measurements of the steady state rates of creatine kinase and ATP synthetase in the rat brain. FEBS Lett. 1982; 140:289–292. [PubMed: 6282642]

Shulman RG, Hyder F, Rothman DL. Cerebral energetics and the glycogen shunt: neurochemical basis of functional imaging. Proc Natl Acad Sci U S A. 2001; 98:6417–6422. [PubMed: 11344262]

Shulman RG, Rothman DL, Behar KL, Hyder F. Energetic basis of brain activity: implications for neuroimaging. Trends Neurosci. 2004; 27:489–495. [PubMed: 15271497]

Siesjo, BK. Brain energy metabolism. Wiley; New York: 1978.

Smith SM. Fast robust automated brain extraction. Hum Brain Mapp. 2002; 17:143–155. [PubMed: 12391568]

Vaishnavi SN, Vlassenko AG, Rundle MM, Snyder AZ, Mintun MA, Raichle ME. Regional aerobic glycolysis in the human brain. Proc Natl Acad Sci U S A. 2010; 107:17757–17762. [PubMed: 20837536]

Vanhamme L, van den Boogaart A, Van Huffel S. Improved method for accurate and efficient quantification of MRS data with use of prior knowledge. J Magn Reson. 1997; 129:35–43. [PubMed: 9405214]

Vaughan JT, Hetherington HP, Otu JO, Pan JW, Pohost GM. High frequency volume coils for clinical NMR imaging and spectroscopy. Magn Reson Med. 1994; 32:206–218. [PubMed: 7968443]

Wallimann T, Wyss M, Brdiczka D, Nicolay K, Eppenberger HM. Intracellular compartmentation, structure and function of creatine kinase isoenzymes in tissues with high and fluctuating energy demands: the ‘phosphocreatine circuit’ for cellular energy homeostasis. Biochem J. 1992; 281(Pt 1):21–40. [PubMed: 1731757]

Wong-Riley MT, Tripathi SC, Trusk TC, Hoppe DA. Effect of retinal impulse blockage on cytochrome oxidase-rich zones in the macaque striate cortex: I. Quantitative electron-microscopic (EM) analysis of neurons. Vis Neurosci. 1989; 2:483–497. [PubMed: 2562109]

Xiong Q, Du F, Zhu XH, Zhang P, Suntharalingam P, Ippolito J, Kamdar FD, Chen W, Zhang J. ATP production rate via CK or ATP synthase in vivo: a novel superfast magnetization saturation transfer method. Circulation Research. 2011

Zhang K, Sejnowski TJ. A universal scaling law between gray matter and white matter of cerebral cortex. Proc Natl Acad Sci U S A. 2000; 97:5621–5626. [PubMed: 10792049]

Zhang XL, Zhu XH, Qiao HY, Liu HY, Vaughan JT, Ugurbil K, Chen W. A circular-polarized double-tuned (^{31}P and ^{1}H) TEM coil for human head MRI/MRS at 7T. Proc. Intl. Soc. Mag. Reson. Med., Toronto. 2003:423.

Zhang Y, Brady M, Smith S. Segmentation of brain MR images through a hidden Markov random field model and the expectation-maximization algorithm. IEEE Trans Med Imaging. 2001; 20:45–57. [PubMed: 11293691]

Zhu XH, Du F, Zhang N, Zhang Y, Lei H, Zhang X, Qiao H, Ugurbil K, Chen W. Advanced *In Vivo* Heteronuclear MRS Approaches for Studying Brain Bioenergetics Driven by Mitochondria. Methods Mol Biol. 2009; 489:317–357. [PubMed: 18839099]

Zhu XH, Zhang Y, Tian RX, Lei H, Zhang N, Zhang X, Merkle H, Ugurbil K, Chen W. Development of ^{17}O NMR approach for fast imaging of cerebral metabolic rate of oxygen in rat brain at high field. Proc Natl Acad Sci U S A. 2002; 99:13194–13199. [PubMed: 12242341]

Highlights

- The ATP utilization rate is three times higher in GM than WM in the human brain
- The majority of the cerebral ATP energy is utilized by neurons in the human brain
- 4.7 billion ATP molecules are utilized by a single cortical neuron per second in humans
- A resting-state human brain utilizes ~5.7 kg ATP/day, 5 times of the brain weight.

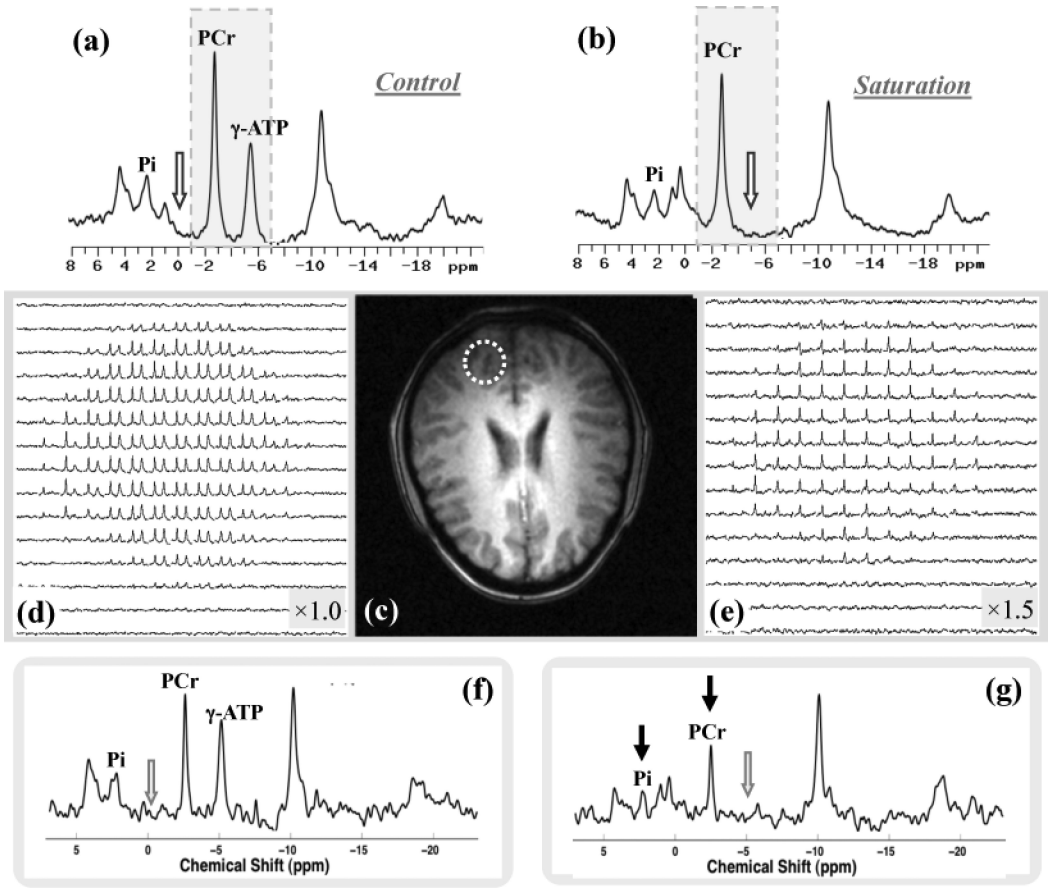

Figure 1.

Measurement of *in vivo* ^{31}P-MT CSI of Human Brain at 7T. Global *in vivo* ^{31}P MR spectra (4 signal averages and TR = 7.1 s) acquired from a representative human brain in the (a) absence (control) and (b) presence (saturation) of γ-ATP. The arrows indicate the saturation site and the shaded areas are the chemical shift range for displaying the ^{31}P-MT CSI spectra used in (d) and (e). (c) A ^{1}H anatomic image and the corresponding 2D ^{31}P-MT CSI slice taken from the 3D data set (TR=0.73 s; 47.3 min data acquisition) from the same subject at control (d) and saturation (e) conditions, respectively. A typical ^{31}P-MT CSI spectrum from a grey-matter dominated voxel (cylindrical voxel shape with actual size of 10.9 ml and nominal size of 2.3 ml) defined by the white circle in (c) at control (f) and saturation condition (g). The solid arrows point to the signal reductions of PCr and Pi compared to the control spectrum due to the chemical exchange and MT effects.

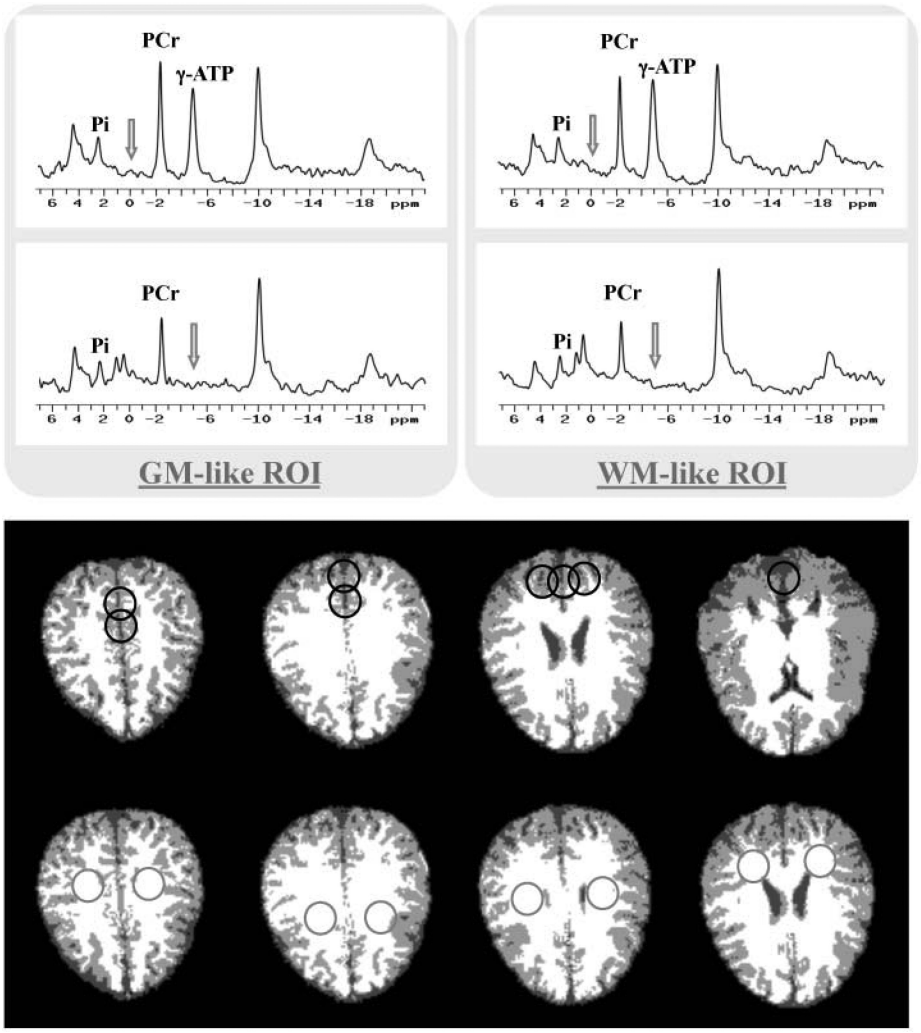

Figure 2.

Three-dimensional Imaging of CMR_{ATPase} and CMR_{CK} in GM- and WM-like VOIs. (a) ^{31}P-MT spectra of GM-like (left panel) and WM-like (right panel) VOIs from a representative subject's brain. Each VOI contains eight individual voxels located in either grey-matter or white-matter dominated brain regions; and each ^{31}P spectrum is the sum of eight spectra from the corresponding voxels of the 3D-CSI data. (b) Segmented ^{1}H MR images of the same subject's brain. Different tissue types, i.e. grey-matter (in light grey color), white-matter (in white color) and CSF (in dark grey color) are identified and displayed in the composition images. The selections of GM-like VOI (black circles in top row) and WM-like VOI (grey circles in bottom row) are also illustrated.

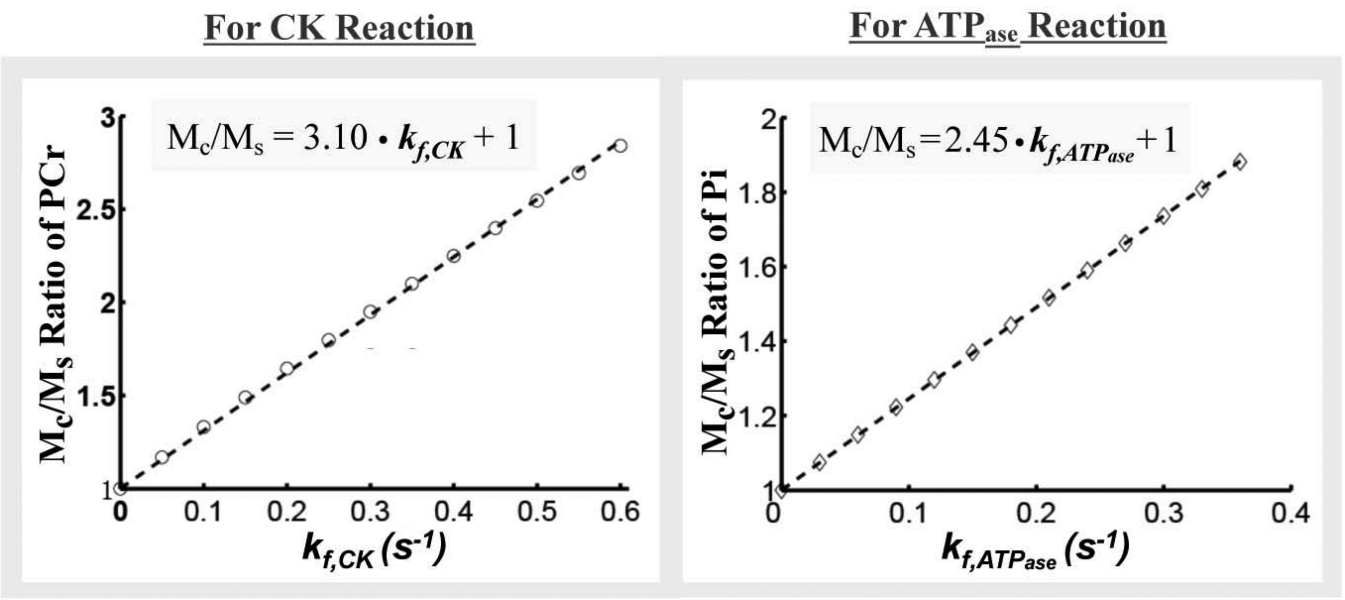

Figure 3.

Simulation Results in Determining T_1^{nom} Values for ATPase and CK Reactions. Simulation (open symbols) and linear regression (dash lines) of the magnetization ratio (M_c/M_s) vs. forward rate constant (k_f) for the CK reaction (a) and ATP_{ase} reaction (b) based on the Bloch-McConnell equations and known values of TR (0.73s), flip angle (36°) and intrinsic T_1 of PCr (4.9s) and Pi (3.7s). The correlation coefficients for both cases are close to 1 (R^2>0.999). The slopes (T_1^{nom}) are 3.10s and 2.45s for PCr and Pi, respectively.

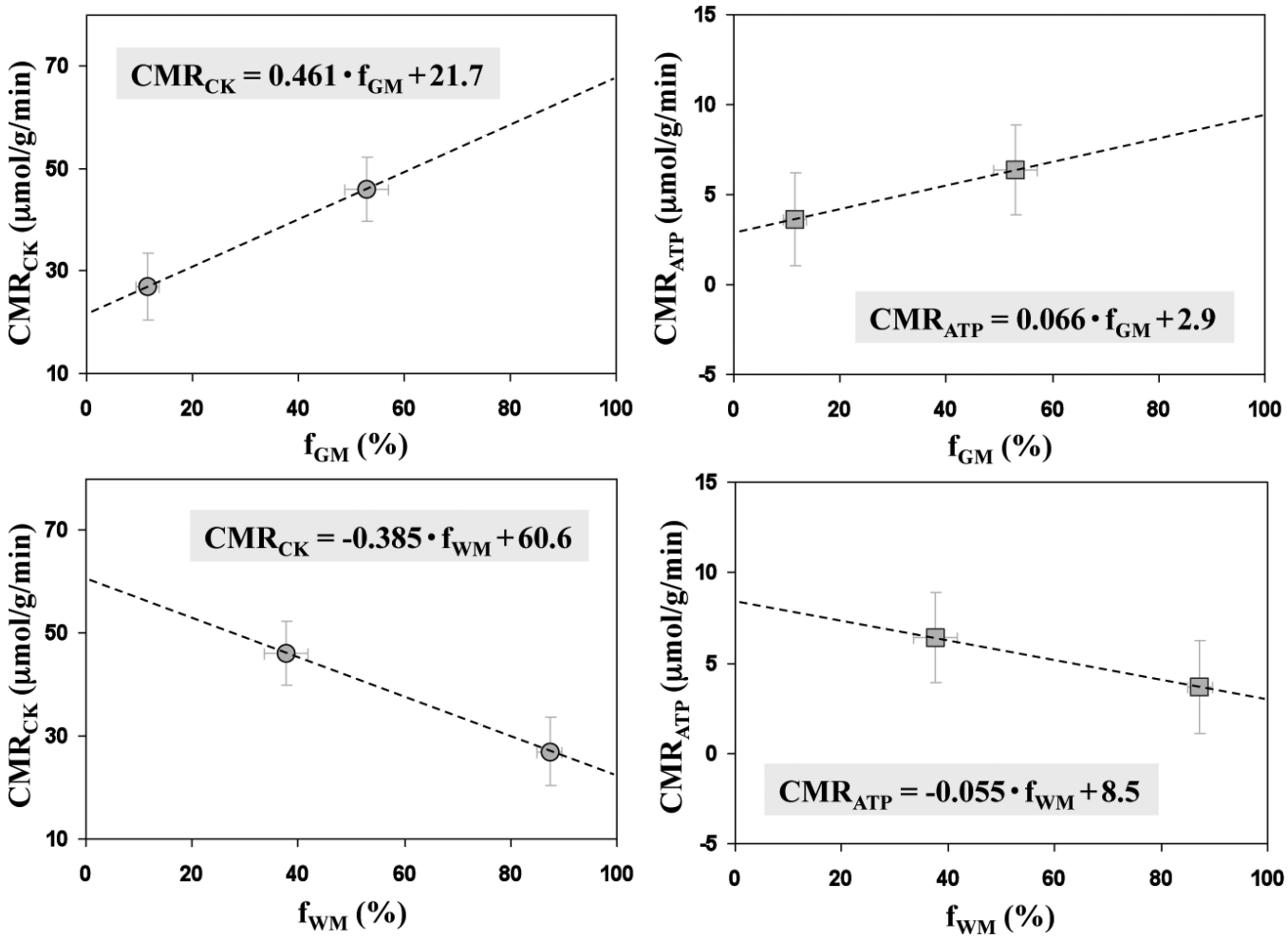

Figure 4.

Quantification of CMR_{ATPase} and CMR_{CK} in Human GM and WM. Linear regression to determine the CMR_{CK} and CMR_{ATPase} values in pure GM and WM tissues of the human brain. The values are 68.8±13.3 and 22.2±7.5 μmol/g/min for $CMR_{CK,GM}$ and $CMR_{CK,WM}$, 9.5±3.4 and 3.0±2.3 μmol/g/min for $CMR_{ATPase,GM}$ and $CMR_{ATPase,WM}$, respectively.

Table 1

Summarized results of tissue composition, metabolite content, reaction rate constant and flux in human brain.

ROI (n=7)	** f_{WM} (%)	** f_{GM} (%)	Pi (mM)	** PCr (mM)	* $k_{f,ATPase}$(S^{-1})	** $k_{f,CK}$ (S^{-1})	* CMR_{ATPase} (µmol/g/min)	** CMR_{CK} (µmol/g/min)
GM-like	37.7 ± 6.3	52.9 ± 4.1	0.93 ± 0.11	2.97 ± 0.11	0.13 ± 0.05	0.28 ± 0.04	6.4 ± 2.5	46.1 ± 6.2
WM-like	87.3 ± 2.8	11.5 ± 2.3	0.96 ± 0.10 #	2.42 ± 0.26	0.09 ± 0.07 #	0.20 ± 0.04	3.7 ± 2.6 #	27.0 ± 6.6

* Two-tail t-test shows $P \leq 0.05$

** Two-tail t-test shows $P < 0.001$

Number of measurement used for calculation was 6.

Table 2

Summary of CMRATPase results in healthy human brain directly measured by 31P-MT method and indirectly estimated from PET or 13C MRS measurements.

Study	Method	Brain Region	Measured Parameter	CMR_{ATPase} (μmol/g/min)
Present Study	^{31}P-MT CSI	Global	CMR_{ATPase}	6.4
Fox et al., 1988	^{15}O PET	Global	$CMRO_2$ [a]	7.5
Ito et al., 2004	^{15}O PET	Global	$CMRO_2$ [a]	6.8
Fox et al., 1988	^{18}F PET	Global	CMR_{glc} [b]	10.2
Lei et al., 2003	^{31}P-MT MRS	Visual	CMR_{ATPase}	12.1 (8.3) [d]
Du et al., 2007	^{31}P-MT MRS	Visual	CMR_{ATPase}	8.8
Fox et al., 1988	^{15}O PET	Visual	$CMRO_2$ [a]	8.5
Fox et al., 1988	^{18}F PET	Visual	CMR_{glc} [b]	11.5
Shen et al., 1999	^{13}C MRS	Occipital-Parietal	V_{TCA} [c]	10.6
Gruetter et al., 2001	^{13}C MRS	Occipital-Parietal	V_{TCA} [c]	8.6
Boumezbeur et al., 2010	^{13}C MRS	Occipital-Parietal	V_{tca} [c]	8.9

[a] P/O ratio of 2.5 is used to estimate CMR_{ATPase} values from $CMRO_2$ (Hinkle PC, 2005).

[b] OGI value of 5.5 and P/O ratio of 2.5 are used to estimate CMR_{ATPase} values from the CMR_{glc} (Vaishnavi et al., 2010; Shulman et al., 2001).

[c] $CMR_{glc}=0.5V_{TCA}$, OGI=5.5 and P/O=2.5 are used to estimate CMR_{ATPase} values from the V_{TCA} (Rothman et al., 2011).

[d] CMR_{ATPase} value in parentheses is calculated based on intracellular Pi concentration of 0.9 mM (Du et al., 2007).